Available online at www.sciencedirect.com

ScienceDirect

journal homepage: www.jfda-online.com

Original Article

Systematically characterize the substance basis of *Jinzhen* oral liquid and their pharmacological mechanism using UPLC-Q-TOF/MS combined with network pharmacology analysis

Jing-Yan Guo [a], *Dong-Mei Wang* [a], *Meng-Jiao Wang* [a], *Jun Zhou* [b], *Ying-Ni Pan* [a,**], *Zheng-Zhong Wang* [b], *Wei Xiao* [c], *Xiao-Qiu Liu* [a,*]

[a] *Department of Traditional Chinese Medicine, Shenyang Pharmaceutical University, 103 Wenhua Road, Shenyang District, Shenyang, Liaoning, 110016, PR China*

[b] *Jiangsu Kanion Pharmaceutical Company Ltd., Lianyungang 222001, PR China*

[c] *State Key Laboratory of New-tech for Chinese Medicine Pharmaceutical Process, Lianyungang 222001, PR China*

ARTICLE INFO

Article history:
Received 10 January 2019
Received in revised form
29 April 2019
Accepted 3 May 2019
Available online 26 June 2019

Keywords:
Metabolic research
TCM
Network pharmacology

ABSTRACT

Jinzhen oral liquid (JZ) is a classical traditional Chinese medicine formula used for the treatment of children lung disease. However, the effective substance of JZ is still unclear. In this study, we used lung injury rat model to study the protective effect of JZ, through UPLC-Q-TOF/MS detection coupled with metabolic research and network pharmacology analysis. Fortunately, 31 absorbed prototype constituents and 41 metabolites were identified or tentatively characterized based on UPLC-Q-TOF/MS analysis, and the possible metabolic pathways were hydroxylation, sulfation and glucuronidation. We optimized the data screening in the early stage of network pharmacology by collecting targets based on adsorbed constituents, and further analyzed the main biological processes and pathways. 24 selected core targets were frequently involved in reactive oxygen species metabolic process, dopaminergic synapse pathway and so on, which might play important roles in the mechanisms of JZ for the treatment of lung injury. Overall, the absorbed constituents and their possible metabolic pathways, as well as the absorbed constituent-target-disease network provided insights into the mechanisms of JZ for the treatment of lung injury. Further studies are needed to validate the biological processes and effect pathways of JZ.

* *Corresponding author*. School of Traditional Chinese Medicine, Shenyang Pharmaceutical University, 103 Wenhua Road, Shenyang 110016, PR China. Fax: +86 24 2398 6469.

** *Corresponding author*. School of Traditional Chinese Medicine, Shenyang Pharmaceutical University, 103 Wenhua Road, Shenyang 110016, PR China. Fax: +86 24 2398 6469.

E-mail addresses: panyingni@163.com (Y.-N. Pan), liuxiaoqiu3388@126.com (X.-Q. Liu).

https://doi.org/10.1016/j.jfda.2019.05.007

1. Introduction

Jinzhen oral liquid (JZ), a traditional Chinese medicine (TCM) formula, treats influenza, bronchitis, pneumonia, H1N1, hand foot and mouth disease and SARS in children. It has become the first-line medicine in pediatrics and was listed as a kind of medical insurance for children in China due to its remarkable efficacy. There are eight medical herbs in JZ including Bovis Calculus Artifactus, Fritillariae Ussuriensis Bulbus, Caprae Hircus Cornu, Rhei Radix et Rhizoma, Scutellariae Radix, Glycyrrhizae Radix et Rhizoma, Chloriti Lapis and Gypsum Fibrosum. The main bioactive constituents in JZ such as alkaloids, amino acids, anthraquinones, flavonoids and saponins exhibited significant biological activities including anti-inflammatory, catharsis, heat-clearing and detoxifying.

Recently, researchers paid more attention to quality control and pharmacological mechanisms of JZ. For example, Peng et al. advocated that JZ combined with clarithromycin could kill Mycoplasma pneumoniae and improve pulmonary inflammation [1]. Zong et al. further demonstrated that the therapeutic mechanism of JZ was closely related to inhibiting protein phosphorylation and blocking the inflammatory pathways of NF-κB and MAPK [2]. In addition, the quantitative method of baicalin and glycyrrhizic acid in JZ was improved in our laboratory [3]. However, the determination of absorbed effective substances of JZ and their metabolites in rats are still limited and the metabolism of single Chinese medicine is completely different from the overall effect of the formula as there may be interactions between components. Therefore, it is of great significance to analyze systematically the absorbed constituents in animals and their corresponding target proteins, in order to get a deeper understanding of pharmacological effects and material basis.

TCM, as a major part of complementary and alternative medicine remedies, shows the advantages with little side effect, low cost and low recurring rate. Recent studies have shown that the clinical effect of TCM is the result of the interaction between multiple components and related targets of various diseases [4]. It has great challenge to investigate the pharmacological mechanisms of herbal formula because the numerous compounds act on multiple targets, and it is hard to address this bottleneck by analyzing the compounds solely with traditional methods. Network pharmacology, developed as "disease-gene-target-drug" network model to understand and evaluate the molecular mechanisms of drug from the multi-dimensional perspective, has greatly promoted the mechanistic study of TCM [5]. This approach has advantages in interpreting the synergistic effects of TCM with components and targets. However, many compounds that were not actually absorbed were also considered, while some actually absorbed compounds were screened out because of less absorption and other reasons. Both of these would herein produce false-positive results in the early screening process of network pharmacology. The ingredients *in vivo* and action mechanism of iridoid extracted from Gardeniae Fructus were investigated [6]. The study analyzed the absorbed prototype constituents and their metabolites through LC-MS method, and selected absorbed substances to analyze the mechanism, combining with the network pharmacology. Therefore, this method can decrease the false positive result by using network pharmacological to analysis the absorbed components. Here, the absorbed substances were selected as target compounds and their targets were searched to construct the network.

Consequently, the absorbed prototype constituents and metabolites of JZ in rats were identified by UPLC-Q-TOF/MS technology and the absorbed substances were used to find their related targets and constructed the constituent-target network by Cytoscape 3.6.1. The targets of influenza, bronchitis and pneumonia were also collected by Online Mendelian Inheritance in Man (OMIM) database, Therapeutic Target Database (TTD), DrugBank database and DisGeNET database, which generated the disease-target network. With Cytoscape 3.6.1, two networks were merged and 24 core targets were analyzed to enrich the pathways. All in all, this study is a connection of chemical components, metabolism *in vivo* and network pharmacology of JZ analysis.

2. Materials and method

2.1. Reagents and materials

Bovis Calculus Artifactus, Fritillariae Ussuriensis Bulbus, Caprae Hircus Cornu, Rhei Radix et Rhizoma, Scutellariae Radix, Glycyrrhizae Radix et Rhizoma, Chloriti Lapis and Gypsum Fibrosum were purchased from Anhui Xinsheng traditional Chinese medicine decoction pieces Co., Ltd and were authenticated by Dr. Yingni Pan, Shenyang Pharmaceutical University. liquiritin (LQ), scutellarin (S), liquiritigenin (L), baicalin (B), oroxylin A-7-O-glucuronide (OA), wogonoside (W), baicalein (BL), aloe emodin (AE), wogonin (WN), chrysin (C), rhein (R), oroxylin A (O), glycyrrhizic acid (GLA), cholic acid (CA), hyodeoxycholic acid (HDCA), emodin (E), chenodeoxycholic acid (CDCA), deoxycholic acid (DCA), chrysophanol (CP) and glycyrrhetinic acid (GLY) (purity > 98%) were obtained from Chengdu Pufeide Biological Technology Company, Ltd. (Chengdu, China). JZ was supplied by Jiangsu Kanion Pharmaceutical Company Ltd. (batch: 180146). Ultra-pure water was prepared with a Milli-Q water purification system (Bedford, France). Acetonitrile and methanol were of UPLC grade from E. Merck (Darmstadt Germany). Other reagents were of analytical grade.

2.2. Preparation of sample solution

JZ was mixed with water at a ratio of 1: 24 (v/v) and then filtered with 0.22 μm filter membrane, afterwards the continued filtrate was used as the sample for UPLC-Q-TOF/MS analysis.

The self-made JZ was prepared according to the preparation process of Chinese Pharmacopoeia (2015 edition). The volume of concentrated solution was one tenth of the original volume.

2.3. Animals experiments

12 male Sprague–Dawley rats (220 ± 20 g) were obtained from Animal Experimental Center of Shenyang Pharmaceutical

University (Shenyang, China) (SCXK (Liao) 2017-0001) and the experimental protocol was in accordance with the Animal Ethics Committee of Shenyang Pharmaceutical University. The rats were maintained in a room with controlled temperature (22–26 °C) and humidity (40%–70%) with a 12 h light–dark cycle. All animals were acclimatized for 1 week before the experiment was started. Diet was prohibited for 12 h prior to the experiment while water was taken freely. Blood samples (0.5 mL each time) were collected from the infraorbital vein and placed in heparinized Eppendorf tubes before administration and at 0, 0.25, 1, 2, 4, 8, 12, 24, 36, and 48 h after intragastric administration of self-made JZ. Then each blood sample was centrifuged for 10 min at 3500 rpm to obtain plasma. Plasma samples were immediately stored at −80 °C. 0–2, 2–4, 4–8, 12–24, 24–36 and 36–48 h urine and 0–24, 24–48 h feces were collected in individual metabolic cages after intragastric administration and the urine was mixed according to the volume ratio of each time interval and stored at −80 °C. The feces samples were grinded after drying in a low-temperature place and then mixed according to the weight ratio of each time period and stored at −80 °C. Bile samples (10 mL in total) were collected for 0–2, 2–4, 4–8, 8–12, 12–24 h and 24–36 h through a plastic cannula surgically inserted into the bile ducts, and then also stored at −80 °C. Rats were given 5% glucose aqueous solution freely in the process of collecting urine, feces and bile.

Rat plasma samples were thawed at 4 °C and centrifuged at 3500 rpm for 10 min. The 200 μL of blank and treated plasma samples were collected and then protein was precipitated by acetonitrile in the ratio of 1:3 (v/v). After 1 min of eddy, the plasma was centrifuged at 13000 rpm for 10 min and the supernatant was collected. The supernatant was dried by nitrogen gas at room temperature, and then the residue was dissolved in 100 μL methanol. After centrifuging for 5 min at 13000 rpm, the supernatant was injected in 5 μL for UPLC-Q-TOF/MS analysis.

Bond-Elut C_{18} solid phase extraction column (500 mg, 3 mL) was activated by 3 mL methanol elution and then eluted by 3 mL water. Rat urine and bile samples were thawed at 4 °C and centrifuged at 3500 rpm for 10 min. The blank and treated samples were collected at 200 μL respectively and extracted on the treated C_{18} solid phase extraction column. The samples were washed with 2 mL water, and then eluted with 2 mL methanol (30 drops/min). Methanol eluent was collected, dried with N_2, and the residue was dissolved in 100 μL methanol. After centrifuging 3500 rpm for 5 min, the supernatant was extracted to automatic sampling vial, and injected with 5 μL for UPLC-Q-TOF/MS analysis.

Blank and treated feces samples (1 g) were extracted with 10 mL methanol and then eddied for 1 min. After ultrasonic extraction for 20 min, 0.22 μm membrane was used to extract the continuous filtrate and 5 μL filtrate was injected for UPLC-Q-TOF/MS analysis.

2.4. UPLC-Q-TOF/MS analysis

Each sample was analyzed on a Waters ACQUITY UPLC system (Milford, MA, USA) equipped with an Agilent UPLC column (ZORBAX Extent-C_{18} 50 mm × 2.1 mm, 1.8 μm). The mobile phase system composed of 0.1% formic acid in water (A) and acetonitrile (B). The flow rate was controlled at 0.3 mL/min with a gradient program of 0–8 min, 5–30% B; 8–16 min, 30–32% B; 16–20 min, 32–40% B; 20–25 min; 40–90% B; 25–28 min, 90-5% B.

The electrospray ionization (ESI) was used as the ionization source by Agilent 6385UHD Accurate-Mass Q-TOF/MS G2 High Definition Mass Spectrometer. The separation was performed by an Agilent orbax Extend-C_{18} Column (2.1 mm × 50 mm, 1.8 μm) at 35 °C. In ESI-MS analysis, the parameters were set as source temperature at 120 °C, and desolvation gas temperature at 350 °C. In positive ion mode, the cone voltage was set as 40 V, the capillary voltage was set as 4.0 kV and the extraction cone voltage was set as 4.0 V. In negative ion mode, the cone voltage was set as 30 V, the capillary voltage was set as 3.5 kV and the extraction cone voltage was set as 5.0 V. To obtain the fragment information of the metabolites, argon was used as the collision gas in MS/MS mode and the collision energy was operated at alternative voltages of 10–70 eV. The mass data were analyzed by Agilent Mass Hunter Workstation software (version B.03.01).

2.5. Data analysis

All data were presented as mean ± standard deviation (S.D.). Statistical analysis was carried out using independent sample t-test by SPSS 19.0(SPSS Inc., Chicago, IL, USA) and the results were considered statistically significant when $P < 0.05$.

2.6. Network construction

The targets of absorbed constituents were obtained from STITCH database (http://stitch.embl.de/, ver.4.0) and SwissTargetPrediction database (http://www.swisstargetprediction.ch/). STITCH is a resource to integrate interactions among metabolic pathways, crystal structures, and drug–target relationships. In this study, the search species was limited as “Homo sapiens”, and the interactions were set as no more than 50 [7]. SwissTargetPrediction is a web server to accurately predict the targets of bioactive molecules based on a combination of 2D and 3D similarity measures with known ligands [8]. The organism was chosen as “Homo sapiens”, then 15 targets of each absorbed constituent and the metabolite were got.

The previous studies have proved that the treatment of JZ is associated with influenza, pneumonia and bronchitis. Therefore the related targets were gathered from the Therapeutic target database (TTD) (https://db.idrblab.org/ttd/), Online Mendelian Inheritance in Man (OMIM) database, DisGeNET database (http://www.disgenet.org/) and DrugBank database (http://redpoll.pharmacy.ualberta.ca/drugbank/). TTD could provide comprehensive information about the clinical trial drugs, targets and pathways [9]. Online Mendelian Inheritance in Man (OMIM) is a comprehensive, authoritative and timely knowledge-base of human genes and genetic disorders compiled to support human genetics research and education and the practice of clinical genetics [10]. DisGeNET is a comprehensive discovery platform designed to address a variety of questions concerning the genetic underpinning of human diseases [11]. The DrugBank database contains more than 4100 drug entries, and more than 14 000 proteins or drug

target sequences linked to these drug entries [12]. A total of 89 bronchitis targets, 161 influenza targets and 105 pneumonia targets were gathered.

To find out the main functions of the 24 core targets of JZ, a Gene Ontology (GO) analysis was performed to gather the corresponding biological processes via the Diversity Visualization Integrated Database (DAVID 6.8 (http://david.abcc.ncifcrf.gov) [13]. Terms with $P < 0.01$ were collected and grouped into clusters based on their membership similarities.

Kyoto Encyclopedia of Genes and Genomes database (KEGG) is a database resource for understanding high-level functions and utilities of the biological system from molecular-level information. We found out the pathway of core targets and got 55 pathways with $P < 0.05$.

3. Result and discussion

3.1. *Identification of chemical constituents in JZ by LC-MS*

Some different constituents in JZ have the same molecular weight, such as chrysin in Scutellariae Radix and chrysophanol in Rhei Radix et Rhizoma (The molecular formulas are both $C_{15}H_{10}O_4$, $[M-H]^-$ theoretical values are both 253.0605). Thus, the retention time and mass spectrometric fragmentation of the reference substances of the main constituents in JZ were analyzed in detail, which was convenient for the subsequent composition analysis. The UPLC-Q-TOF/MS positive and negative ion flow pattern of mixed reference solution were shown in Fig. 1a,b, and its main mass spectra were shown in Table 1.

Afterwards, JZ sample solution was injected and analyzed by UPLC-Q-TOF/MS. The total ion flow chromotogram of JZ was obtained (Fig. 1c,d). The chemical constituents in JZ were identified by comparing the information given by mass spectrometry with those in the reference. A total of 63 chromatographic peaks were detected in the sample of JZ, and the relevant mass spectrum data were shown in Table S1. 51 chromatographic peaks were detected under negative ion mode. Among them, 19 were from Glycyrrhizae Radix et Rhizoma, 11 were from Scutellariae Radix, 10 were from Bovis Calculus Artifactus, 5 were from Fritillariae Ussuriensis Bulbus, 6 were unknown components, and 5 were from sweetener, including J33, J36, J38, J39 and J44. Among them, J33 was stevioside. In the positive ion mode, 12 constituents were identified, all from Fritillariae Ussuriensis Bulbus.

3.2. *Characterization of the absorbed prototype constituents and the detection and identification of the metabolites*

After analyzed the plasma, bile, urine and fecal samples of rats after intragastric administration of self-made JZ, the mass spectra of UPLC-Q-TOF/MS biological samples were obtained (Fig. 2). 72 substances were detected in combination with the common metabolic pathways *in vivo* and the informations reported in relevant literature by comparing the information given by mass spectrometry with the information of reference substances and the related chemical constituents of JZ. Of the 72 substances, 31 were prototype constituents, among which 11 were from Glycyrrhizae Radix et Rhizoma, 5 were from Scutellariae Radix, 7 were from Bovis Calculus Artifactus, 5 were from Fritillariae Ussuriensis Bulbus and 3 were unknown prototype constituents (M1, M40, M45); 41 were metabolites, of which 23 were from Glycyrrhizae Radix et Rhizoma, 12 were from Scutellariae Radix and 6 were from Rhei Radix et Rhizoma. The related mass spectrometry data were listed in Table 2.

There were still some unknown compounds which cannot be identified by LC-MS. NMR spectroscopy is very useful for structure elucidation, and HPLC-SPE-NMR has been applied in identifying compounds, like rapid analysis of isoflavonoids from the roots of *Smirnowia iranica* [14] and identification of metabolites of TCM prescription Sinisan in miniature pig urine via intragastric administration [15]. With the help of HPLC-SPE-NMR, these ambiguous structures in JZ may be clarified. As the technology of HPLC-NMR has not been widely used, it has not been done in this study.

3.3. *Possible metabolic routes of the prototype constituents*

According to the mass spectrometry information, the prototype constituents and metabolites were preliminarily analyzed, and it was found that most prototype constituents underwent hydroxylation, sulfation and glucuronidation. Only the constituents of Glycyrrhizae Radix et Rhizoma and Scutellariae Radix produced both of prototype constituents and metabolites, and Glycyrrhizae Radix et Rhizoma had the most prototypes constituents and metabolites. So the metabolic pathways of Glycyrrhizae Radix et Rhizoma were selected as an example. The Fig. 3 illustrated the main metabolites and the possible metabolic routes of the absorbed constituents of Glycyrrhizae Radix et Rhizoma.

3.4. *Network analysis*

3.4.1. *The absorbed constituent-related target network and disease-related target network*

We searched relevant targets of 72 constituents and got 1357 results. After inputting these data into Cytoscape 3.6.1, absorbed constituent-target network was got as shown in Fig. S1. After analyzing the four important topological properties of "degree", "betweenness", "closeness", and "coreness", we found that isoliquiritin, emodin, liquiritigenin, rhein, baicalin, glycochenodeoxycholic acid, wogonoside aceylation and wogonin connected more targets and might show greater biological activities and therapeutic effects of JZ *in vivo*. From the predicted targets of the 72 main constituents, MAPT, TDP1, AKR1B10, AKR1B1 and AKR1B15 were topological important. MAPK3 (Mitogen-activated protein kinase3) was found closely related to the mechanism of JZ in the treatment of acute lung injury [2]. TDP1 is a repair gene capable of resolving both oxidative damage and topoisomerase I (Top1)-mediated damage to DNA in eukaryotic cells, which is closely related to primary lung cancer [16]. A human member of the aldo-keto reductase (AKR) superfamily, AKR1B10, which exhibits high sequence identity with human aldo-keto reductase (AKR1B1) is identified as a biomarker of lung cancer [17]. Human aldo-keto reductase 1B15 (AKR1B15), a newly discovered enzyme

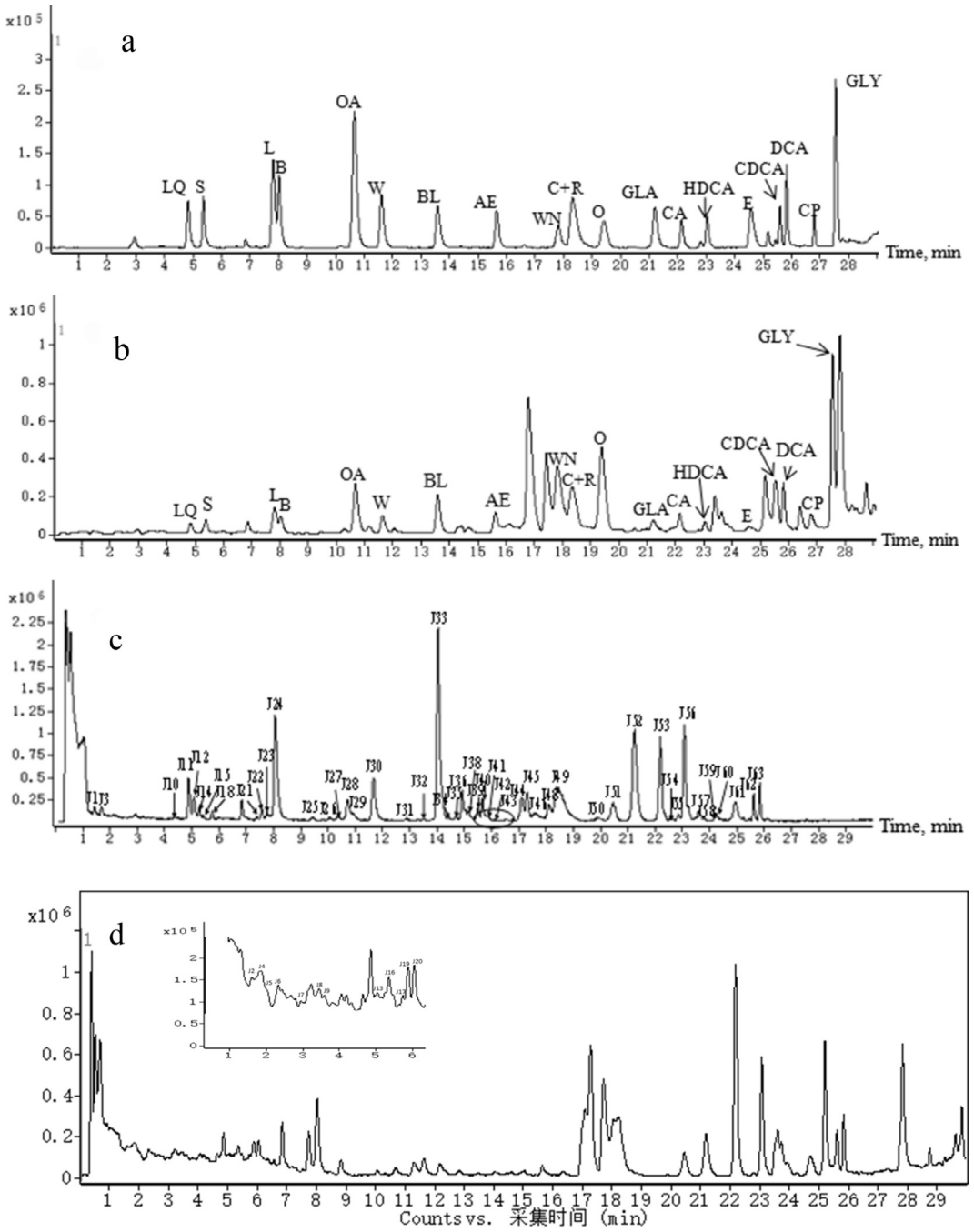

Fig. 1 – UPLC-Q-TOF/MS total ion flow chromatography of mixed reference solution (a-negative, b-positive), UPLC-Q-TOF/MS total ion chromatograms of JZ under negative (c) and positive (d) ion mode.

that shares 92% amino acid sequence identity with AKR1B10 also showed higher catalytic activity than AKR1B10 [18].

We searched the targets of the three diseases from OMIM, TTD, DisGeNET and DrugBank, and got 89 targets relative with bronchitis, 105 targets relative with pneumonia and 161 targets relative with influenza. After inputting these data into Cytoscape 3.6.1, the network was obtained as shown in Fig. S2.

3.4.2. *The absorbed constituent-target-disease network construction*

To establish the relationship of constituents, relative targets and the three diseases, we merged the two networks by Cytoscape 3.6.1 and got 24 main targets. In order to get a better perspective, we selected overlapping targets of the diseases and the 72 constituents, and their related compounds as well as diseases to merge a new constituent-target-disease network. The result was shown in Fig. 4a.

In the network, the compounds with all the top 10 values of degree, betweenness and closeness were glycochenodeoxycholic acid, taurocholic acid, 22β-acetoxylglycyrrhizin-2gluA + O and pingpeimine which belonged to Bovis Calculus Artifactus, Glycyrrhizae Radix et Rhizoma and Fritillariae Ussuriensis Bulbus. And the targets with the top 4 were ADORA1, HSD11B1, PTGS1, and NR3C1. It was found that

Table 1 – Accurate mass measurements of deprotonated molecular and fragment ions of reference substances.

Substances	t_R (min)	Formula	(–)ESI-MS		(+)ESI-MS		(–)ESI-MS^2
			Measure mass $[M-H]^-$ (*m/z*)	Error (ppm)	Measure mass $[M+H]^+$ (*m/z*)	Error (ppm)	Fragment ions (*m/z*)
LQ	4.88	$C_{21}H_{22}O_9$	417.1192	0.02	441.1192 $[M+Na]^+$	−2.30	255.0644, 135.0075, 119.0496
S	5.40	$C_{21}H_{18}O_{12}$	461.0722	−0.07	463.0884	−2.76	285.0374
L	7.89	$C_{15}H_{12}O_4$	255.0658	−0.20	257.0817	−3.36	135.0093, 119.0507
B	8.06	$C_{21}H_{18}O_{11}$	445.0782	0.13	447.0943	−4.31	269.0446
OA	10.71	$C_{22}H_{20}O_{11}$	459.0935	0.04	461.1103	−5.06	283.0612
W	11.67	$C_{22}H_{20}O_{11}$	459.0928	−0.11	461.1102	−5.21	283.0613, 268.0366
BL	13.59	$C_{15}H_{10}O_5$	269.0474	−7.01	271.0619	−6.65	136.9895, 65.0047
AE	15.69	$C_{15}H_{10}O_5$	269.0468	−4.72	271.0613	−4.51	240.0420, 183.0464, 167.0506
WN	17.87	$C_{16}H_{12}O_5$	283.0611	−0.35	285.0769	−3.97	268.0389, 249.1134
CN	18.33	$C_{15}H_{10}O_4$	253.0519	−5.63	255.0665	−4.03	165.0721, 143.0510, 119.0507
R	18.33	$C_{15}H_8O_6$	283.0266	−5.73	285.0410	−5.12	280.9835, 253.0512
O	19.45	$C_{16}H_{12}O_5$	283.0628	−5.75	285.0772	−5.19	215.0632, 125.8745
GLA	21.24	$C_{42}H_{62}O_{16}$	821.3969	0.05	823.4120	+0.49	351.0573, 193.0353, 113.0252
CA	22.18	$C_{24}H_{40}O_5$	407.2800	−0.74	431.2785 $[M+Na]^+$	−4.51	343.2629, 289.2161, 95.0503, 69.0348
HDCA	23.08	$C_{24}H_{40}O_4$	391.2851	−0.08	415.2819 $[M+Na]^+$	+4.33	391.2858
E	24.67	$C_{15}H_{10}O_5$	269.0472	−6.13	271.0612	−4.06	269.0472
CDCA	25.62	$C_{24}H_{40}O_4$	391.2848	−0.15	415.2822 $[M+Na]^+$	+0.72	343.2644, 69.0353
DCA	25.84	$C_{24}H_{40}O_4$	391.2849	−0.13	415.2822 $[M+Na]^+$	−0.05	343.2647, 69.0355
CP	26.79	$C_{15}H_{10}O_4$	253.0527	−7.17	255.0664	−4.54	164.7768
GLY	27.57	$C_{30}H_{46}O_4$	469.3332	−1.67	471.3493	−5.13	368.0387, 265.1493

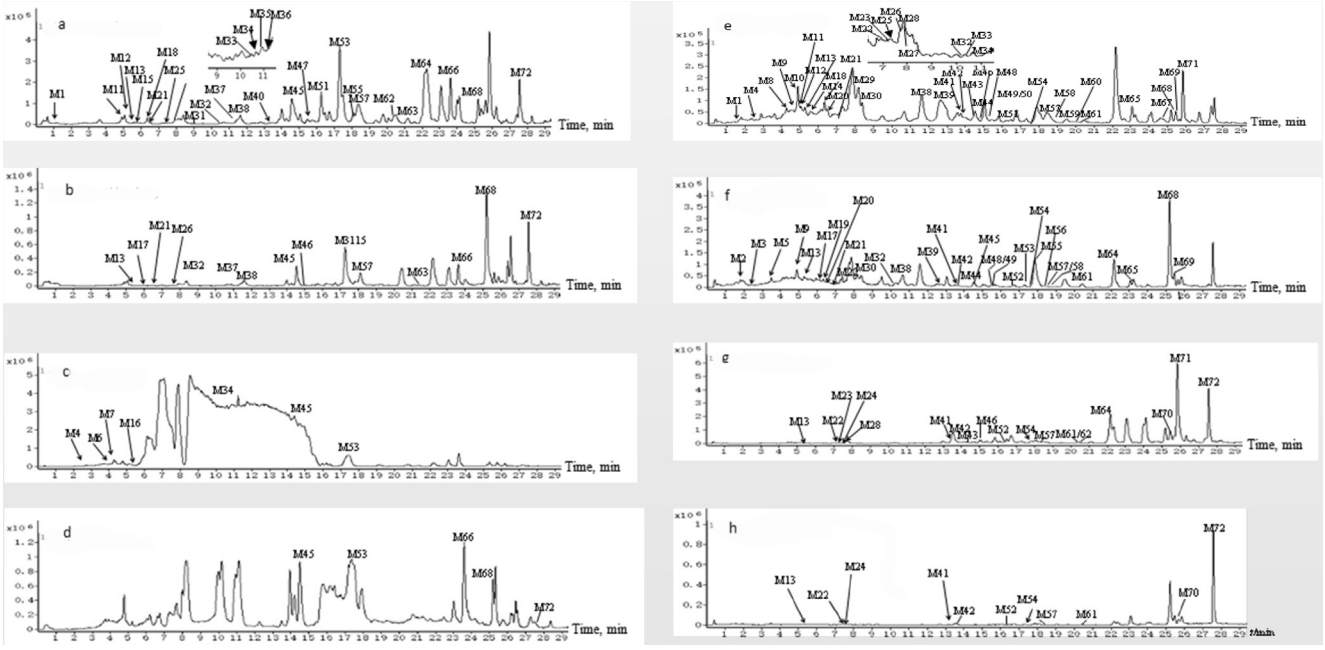

Fig. 2 – The extracted ion chromatograms of metabolites plasma (a-negative, b-positive), bile (c-negative, d-positive), urine (e-negative, f-positive, and fecal (g-negative, h-positive) in JZ.

glycochenodeoxycholic acid could affect the expression of autophagy-related protein in alveolar epithelial cells, impair lysosomal activity and permeability, and may lead to cell death [19]. Taurocholic acid has anti-inflammatory and antitussive effect since ancient times, while pingpeimine is the main active ingredient of Fritillaria, which has anti-inflammatory and antitussive effects. This reminded us that as the metabolite of glycyrrhizin, 22β-acetoxylglycyrrhizin-2gluA + *O* probably also had the ability influenza A virus. 22β-acetoxylglycyrrhizin-2gluA + *O* is a metabolite of glycyrrhizin. Glycyrrhizin is one of the main active compounds of Glycyrrhizae Radix et Rhizoma, and can protect cells from infection with influenza A virus (IAV) [20]. It was inferred that 22β-acetoxylglycyrrhizin-2gluA + *O* probably had the effect of anti-influenza A virus. Ian C. Davis demonstrated that adenosine-mediated neutrophil ADORA1 activation might play an important role in the pathogenesis of lung dysfunction and injury in influenza patients. COX-1 is one of the key enzymes causing inflammation. Alison K. Bauer has investigated COX-1 and COX-2 expression in early, intermediate and late

Table 2 – Accurate mass measurements of deprotonated molecular and fragment ions of metabolites in JZ.

Peak no.	t_R (min)	Formula	(−)ESI-MS		(+)ESI-MS		(−)ESI-MS^2	Identified compound	Source	
			Measure mass $[M-H]^-$ (*m/z*)	Error (ppm)	Measure mass $[M+H]^+$ (*m/z*)	Error (ppm)	Fragment ion (*m/z*)			
M1	1.272	$C_{10}H_{19}NO_5$	232.1039	−2.06	–	–	206.0824, 186.0928, 144.0820, 89.0249	unknown	P, U	p
M2	1.819	$C_{27}H_{43}NO_6$	–	–	478.3186	3.98	–	pingpeimine or its isomer	U	p
M3	2.354	$C_{27}H_{41}NO_5$	–	–	460.3001	0.23	–	verdine or its isomer	U	p
M4	2.784	$C_{27}H_{30}O_{15}$	593.1519	−1.72	–	–	417.1069, 255.0642, 135.0837	liquiritin + gluA	B, U	m
M5	3.49	$C_{27}H_{41}NO_5$	–	–	460.3059	−3.04	–	Verdine or its isomer[56]	U	p
M6	4.091	$C_{21}H_{20}O_{13}S$	511.0522	−0.04	–	–	431.0958, 335.0188, 255.0669, 175.0246	liquiritigenin + gluA + sul	P, B	m
M7	4.282	$C_{21}H_{22}O_{12}S$	497.0789	−6.11	–	–	417.1174, 255.0642, 135.0069, 91.0178	liquiritin + sul	B	m
M8	4.309	$C_{26}H_{28}O_{14}$	563.1456	0.9	565.1573	−6.08	352.9320, 135.0071, 119.0500	isoschaftoside	U	p
M9	4.789	$C_{21}H_{20}O_{10}$	431.1004	0.22	433.1151	−4.73	255.0642, 175.0232, 135.0065 113.0234	liquiritigenin + gluA	U	m
M10	4.877	$C_{21}H_{22}O_9$	417.1199	−3.25	–	–	255.0664, 135.0090, 119.0496	liquiritin[a]	U	p
M11	4.998	$C_{21}H_{20}O_{13}S$	511.0559	−2.26	–	–	335.0287, 255.0633	liquiritigenin + gluA + sul	P, U	m
M12	5.048	$C_{26}H_{30}O_{13}$	549.1615	−6.01	–	–	255.0650	liquirtin apioside	P, U	p
M13	5.252	$C_{26}H_{28}O_{13}$	547.1477	−2.13	549.162	−4.04	457.1164, 367.0986, 337.062	chrysin-6-C- rabinosyl -8-C-glucoside	P, U, F	P
M14	5.574	$C_{27}H_{30}O_{16}$	609.1463	−0.39	–	–	433.1124	isoliquiritin + O + gluA	U	m
M15	5.792	$C_{21}H_{22}O_{12}S$	497.0769	−0.11	–	–	417.1158	liquiritin + Sul	P	m
M16	5.819	$C_{21}H_{18}O_{10}$	429.1972		–	–	253.0630	chrysin-7-O-gluA	B	m
M17	6.053	$C_{27}H_{43}NO_3$	–	–	430.3309	−1.66	–	verticinone	P, U	P
M18	6.318	$C_{21}H_{22}O_9$	417.1194	−0.62	–	–	255.8189	neoisoliquiritin	P, U	m
M19	6.330	$C_{26}H_{41}NO_3$	–	–	416.3164	−1.06	–	pinbeinone	U	p
M20	6.560	$C_{27}H_{26}O_{17}$	621.1118	0.57	623.1265	−1.69	269.0454	baicalin + gluA	U	m
M21	6.585	$C_{27}H_{26}O_{17}$	621.1048	−2.55	623.1263	−3.73	445.0760, 269.0436	emodin-diglucuronides	P, U	m
M22	7.331	$C_{15}H_{10}O_4$	253.0515	−2.59	255.0656	−0.82	135.3940, 117.0323, 91.0177	liquiritigenin-2H	U, F	m
M23	7.345	$C_{26}H_{30}O_{13}$	549.1629		–	–	255.0678, 119.0487	isoliquirtin apioside	U, F	p
M24	7.372	$C_{15}H_{10}O_4$	253.0518	−0.2	255.0656	−1.84	151.0359	baicalein-O	F	m
M25	7.546	$C_{21}H_{22}O_9$	417.1191	−1.7	419.1342	−6.16	255.0654	isoliquiritin	P, U	p
M26	7.821	$C_{21}H_{22}O_{10}$	433.1142	−0.33	–	–	255.0659, 151.0398, 135.0080, 119.0494	isoliquiritin + O	P, U	m
M27	7.830	$C_{15}H_{12}O_4$	255.0665	1.22	257.0823	−6.3	135.0080, 119.0494, 91.0182,	isoliquiritigenin	U	p
M28	7.863	$C_{15}H_{12}O_4$	255.0681	1.22	257.0825	−6.38	135.0093, 119.0507, 91.0200	liquiritigenin[a]	U, F	p
M29	8.147	$C_{15}H_{12}O_7S$	335.0234	−4.95	–	–	255.0636, 135.866, 119.0480	liquiritigenin + gul	U	m
M30	8.197	$C_{21}H_{22}O_{10}$	433.1158	−5.32	435.1292	−1.03	255.0637, 417.1185	isoliquiritin + O	U	m
M31	9.049	$C_{21}H_{20}O_{11}$	447.0955	−2.53	–	–	255.0643, 135.0087, 91.0259	isoliquiritigenin + O + gluA	P	m
M32	10.361	$C_{21}H_{18}O_{10}$	429.0846	−5.02	–	–	253.0494, 113.0229	chrysin-7-O-gluA	P, U	p
M33	10.678	$C_{22}H_{20}O_{12}$	475.0893	−4.46	477.1084	1.6	299.1714	emodic acid-O-gluA	P, U	m
M34	10.738	$C_{22}H_{20}O_{11}$	459.0908	−1.69	461.1091	−2.95	283.0595	oroxylin -7-O-glucuronide[a]	P, B,U	p
M35	10.862	$C_{22}H_{20}O_{12}$	475.0883	−2.48	477.1022	0.32	299.0544	5,6,7-trihydroxy-8-methoxyflavone-7-O-glucuronid	P	m
M36	10.976	$C_{22}H_{20}O_{12}$	475.088	1.28	477.1032	−0.93	445.1095	baicalin + OH + CH_2	P	m
M37	11.355	$C_{21}H_{22}O_{10}$	433.1135	0.38	–	–	255.077	isoliquiritin + O	P	m
M38	11.622	$C_{22}H_{20}O_{11}$	459.0943	−2.98	461.1089	−3.14	283.0613, 268.0366	wogonoside[a]	P, U	p
M39	12.733	$C_{15}H_{14}O_7S$	337.0412	−0.82	339.0533	−3.14	257.08	liquiritigenin+2H + sul	U	m
M40	13.41	$C_{42}H_{62}O_{17}$	837.396		839.4452	–	351.0523, 113.0274	unknown	P	p
M41	13.535	$C_{15}H_{14}O_4$	257.0814	−2.45	259.0972	1.12	151.0394, 93.0349	liquiritigenin+2H	U, F	m

(*continued on next page*)

Table 2 – (*continued*)

Peak no.	t_R (min)	Formula	(−)ESI-MS		(+)ESI-MS		(−)ESI-MS^2	Identified compound	Source	
			Measure mass $[M-H]^-$ (*m/z*)	Error (ppm)	Measure mass $[M+H]^+$ (*m/z*)	Error (ppm)	Fragment ion (*m/z*)			
M42	13.752	$C_{16}H_{12}O_9S$	379.2483		–	–	283.0583	wogonin + OH + sul	U, F	m
M43	14.412	$C_{15}H_{10}O_8S$	349.2026		–	–	269.1513	baicalein + sul	U, F	m
M44	14.521	$C_{15}H_{12}O_4$	255.0669	−2.42	257.0822	−5.67	119.0500, 91.0187	isomer of liquiritigenin	U	m
M45	14.646	$C_{26}H_{41}NO_6$	462.2878	1.38	464.3	1.83	74.0264	unknown	P, B, U	P
M46	15.056	$C_{24}H_{40}O_5$	407.282	−5.72	–	–	343.2657, 325.2542, 243.1742, 69.0343	isomer of cholic acid	P, U, F	P
M47	15.665	$C_{44}H_{64}O_{18}$	879.4036	−2.08	–	–	351.0532, 193.0368	22β− acetoxylglycyrrhizin	P	P
M48	15.692	$C_{15}H_{10}O_5$	269.0439	−0.6	271.0617	−4.3	240.0404, 183.5663, 167.6533	aloe emodin[a]	U	m
M49	15.729	$C_{16}H_{14}O_4$	269.043	−2.95	271.0611	−3.93	–	isoliquiritigenin + CH_2	U	m
M50	15.732	$C_{15}H_{10}O_5$	269.0473	−0.37	–	–	240.0404, 167.6533	isomer of emodin	U	m
M51	16.25	$C_{22}H_{20}O_{13}$	491.2286		–	–	475.1936, 459.0226	wogonoside+2OH	P, U	m
M52	16.463	$C_{42}H_{62}O_{17}$	837.3909		839.4094		351.2158	licorice-saponin G_2	U, F	P
M53	17.353	$C_{26}H_{43}NO_6$	464.3041	−2.44	466.3172	–	74.0249	glycocholic acid	P, B, U	P
M54	17.856	$C_{16}H_{12}O_5$	283.0255	−1.77	–	–	268.0389, 249.1134	wogonin[a]	U, F	P
M55	18.088	$C_{42}H_{62}O_{17}$	837.3931	−4.37	–	–	351.0589, 193.0328	24-hydroxyl-glycyrrhizin	P, U	P
M56	18.327	$C_{15}H_{10}O_4$	253.0506	−0.72	255.0665	−6.68	165.0721, 143.0510, 119.0570	chrysin[a]	U	m
M57	18.372	$C_{26}H_{45}NO_7S$	514.2843	−0.26	–	–	124.0083, 79.9506	taurocholicacid	P, U, F	P
M58	18.566	$C_{15}H_8O_6$	283.0248	−2.46	285.0399	−2.17	253.0512	rhein[a]	U	m
M59	19.764	$C_{16}H_{14}O_5$	285.0747	−6.4	–	–	283.0595	wogonin reduction	U	m
M60	19.967	$C_{16}H_{12}O_8S$	363.0621	−2.5	–	–	283.0598	wogonin + Sul	U	m
M61	20.235	$C_{32}H_{48}O_7$	543.335	−1.76	545.3504	−5.3	501.3245	22β-acetoxylglycyrrhizin-2gluA + *O*	U, F	m
M62	20.26	$C_{24}H_{40}O_5$	407.281	−5.96	–	–	–	hyocholic acid	P, F	p
M63	21.195	$C_{42}H_{62}O_{16}$	821.398	−1.87	–	–	351.0546, 193.0385	glycyrrhizin[a]	P	p
M64	22.599	$C_{24}H_{23}O_{12}$	487.2385		–	–	459.5632, 283.2632	wogonoside aceylation	P, U, F	m
M65	23.125	$C_{24}H_{40}O_4$	391.2851	−0.02	–	—	–	hyodeoxycholic acid[a]	U	P
M66	23.618	$C_{26}H_{43}NO_5$	448.3076	0.48	450.3241	3.81	74.0243	glycochenodeoxycholic acid	P, B	p
M67	24.637	$C_{15}H_{10}O_5$	269.0447	−4.53	271.0612	3.97	241.0473, 225.0555, 197.0610 169.0630	Emodin[a]	U	m
M68	25.355	$C_{36}H_{54}O_{10}$	645.3638	1.63	647.3798	−7.64	469.3311	glycyrrhetinic acid + gluA	P, B, U	m
M69	25.422	$C_{30}H_{46}O_5$	485.3265	−5.67	487.344	−4.58	441.3354	glycyrrhetinic acid + *O*	U	m
M70	25.5	$C_{31}H_{45}O_6$	513.3219	−0.16	515.3375	−2.19	471.3125, 453.3015	22β-acetoxylglycyrrhizin-2gluA-CH_2	F	m
M71	25.836	$C_{24}H_{40}O_4$	391.2836	−1.6	–	–	343.0869	deoxycholic acid[a]	B, U, F	p
M72	27.594	$C_{30}H_{46}O_4$	469.334	−0.03	471.3471	−3	319.4262, 269.0357, 96.9580	glycyrrhetinic acid[a]	P, B, F	m

B: bile, **F:** feces, **P:** plasma, **U:** urine, a:identified by comparing with reference standards. p:parent compounds, m: metabolites.

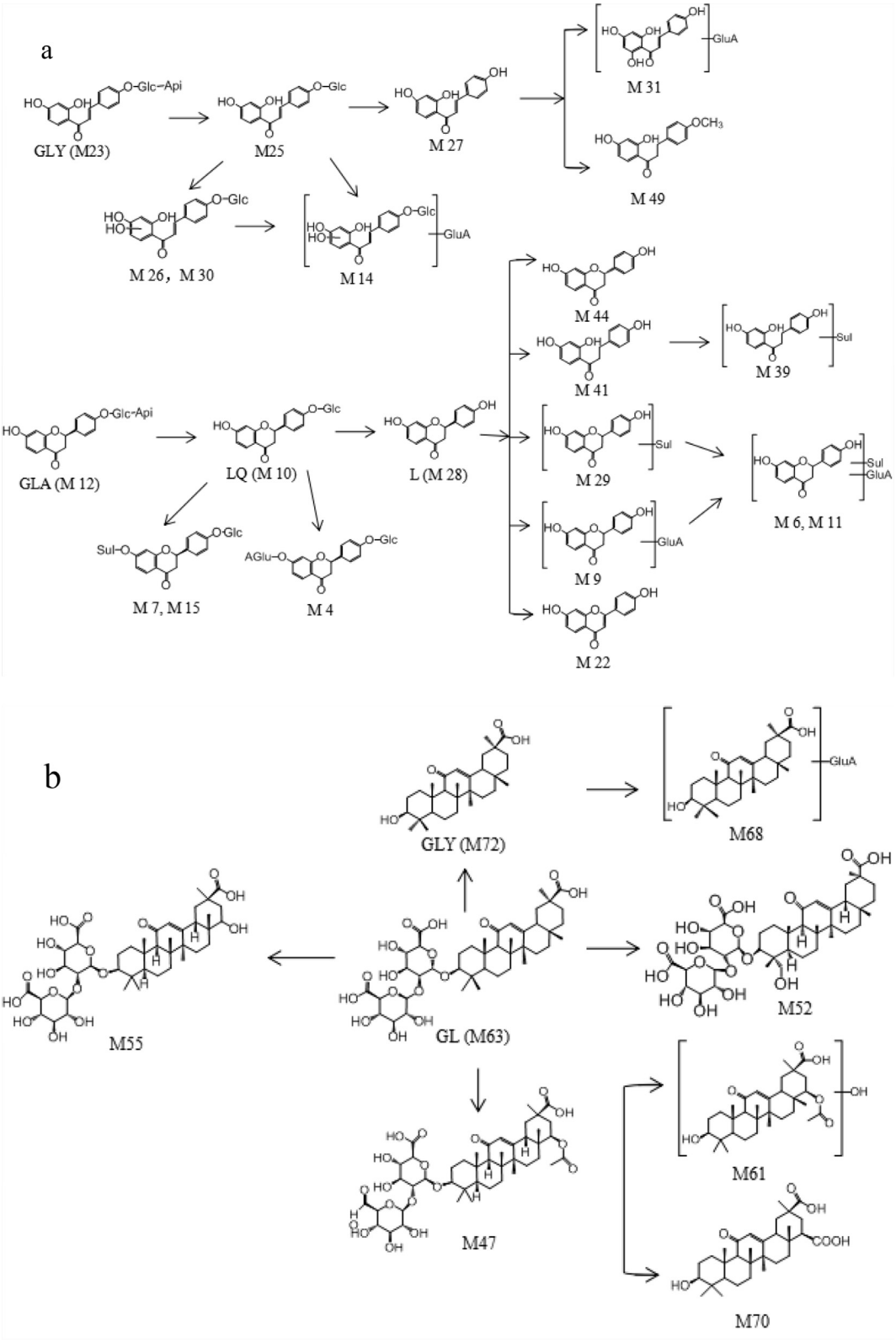

Fig. 3 – a: Proposed metabolic pathways of licorice flavonoids (isoliquirtin apioside, isoliquiritin, isoliquiritigenin, liquirtin apioside, liquiritin and liquiritigenin) in rats; Api, apioside; Glc, glucoside; Sul, sulfate; GluA, glucuronic acid residue. b: Proposed metabolic pathways of glycyrrhizic acid, glycyrrhetinic acid, 24-hydroxyl-glycyrrhizin and 22β-acetoxylglycyrrhizin in rats.

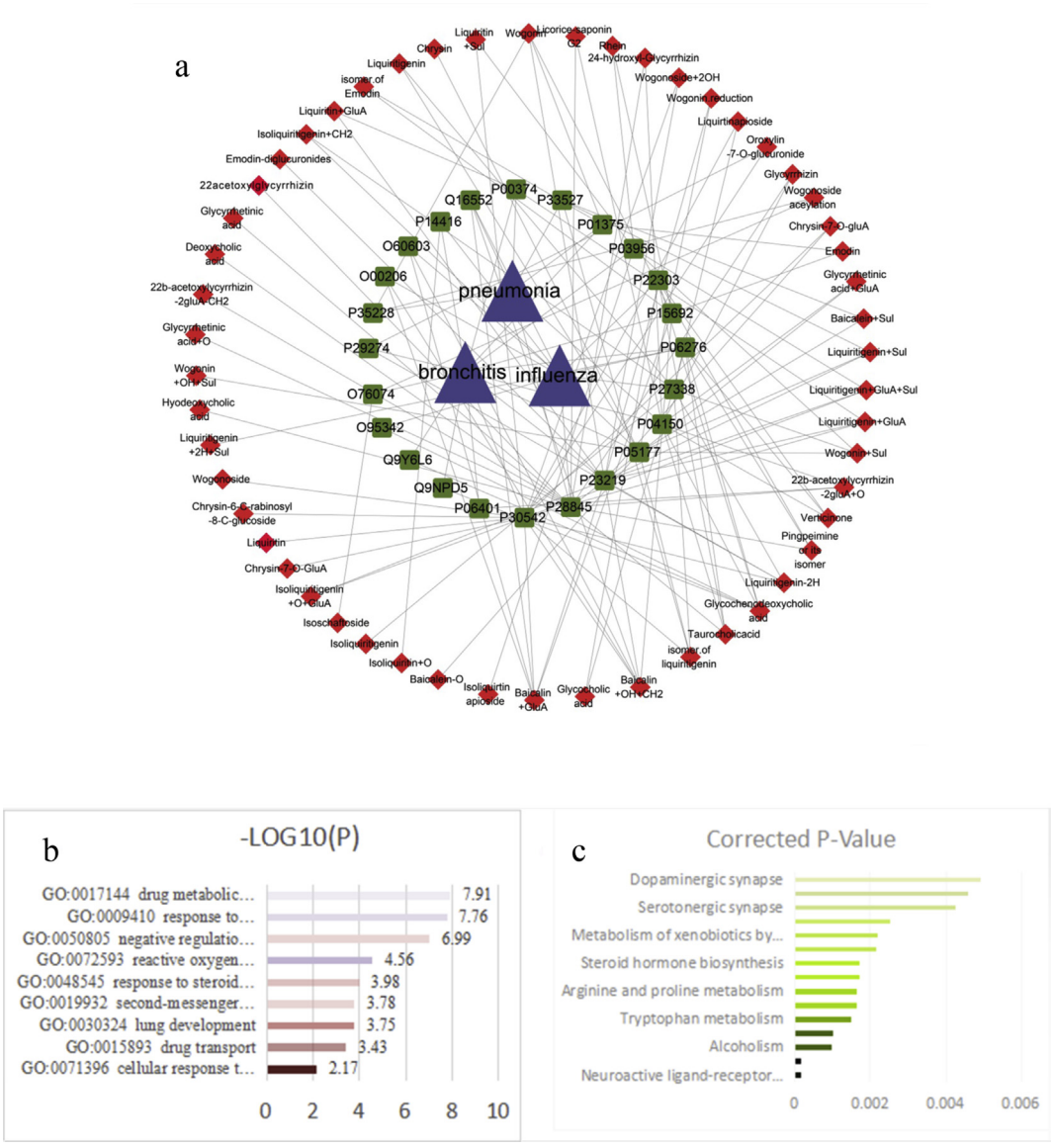

Fig. 4 – The absorbed constituent-target-disease network (a). GOBP analysis of 24 core targets of JZ (b), KEGG pathways analysis of 24 core targets of JZ (c).

stages of tumorigenesis and found staining of COX-1 in the bronchiolar and alveolar epithelia, bronchiolar smooth muscle and alveolar macrophages [21]. To our knowledge, glucocorticoids induce surfactant synthesis in the late foetal lung and deficient its action causes respiratory distress syndrome (RDS). HSD11B1 converts inert cortisone (11-dehydrocorticosterone in rodents) into active cortisol (corticosterone), thus amplifying intracellular GC action [22].

3.4.3. *Bioinformatics enrichment analysis*

To further probe the physiological features of the 24 core targets, we assessed the GOBP enrichment in Metascape (http://metascape.org). Terms with $P < 0.01$ (Table S2) were collected and grouped into clusters based on their membership similarities. The result was shown in Fig. 4b.

The GOBP results showed that JZ might inhibit the inflammatory response of airway epithelial cells by inhibiting the metabolism of reactive oxygen species (ROS) [23], which was regarded as key substances modulating the pulmonary vascular endothelial, and a further study was needed to prove it. Pathogenesis of a number of human diseases including the lung was thought to be interacted with damage to cellular macromolecules like lipids when the production of ROS of the cellular overwhelms its antioxidant capacity, which indicated that cellular response to lipid may show a surprising effect [24]. Intriguingly, xenobiotics metabolism and reactive oxygen species biosynthesis were found to be closely related to COPD small airway epithelial cells [25], which might provide some promising new therapeutic mechanisms of JZ. These three biological processes seem to have some internal connections, further studies were deserved. Steroid hormone is effective in the complex therapy of chronic pneumonia in children [26] and negative autoregulatory feedback loops served to limit hormonal responses. Adenosine deaminase (ADA) is an essential enzyme of purine catabolism, and the metabolic disturbances associated with its deficiency in mice result in

abnormal lung development and the promotion of lung inflammation and damage [27].

With the help of DAVID (https://david.ncifcrf.gov/home.jsp) and KOBAS 3.0 (http://kobas.cbi.pku.edu.cn/), an enrichment of 24 targets' pathways was made by KEGG database. The pathways were ranked by their nominal *P* values with a cut-off of 0.005 (Table S3) in Fig. 4c. The significant KEGG pathways were neuroactive ligand–receptor interaction, metabolic pathways and alcoholism among a total of 15 pathways.

In the result of neuroactive ligand–receptor interaction, JZ may up-regulate DRD1, ADORA1 and NR3C1 by affecting dopamine, adenosine and cortisol. Dopamine receptor agonists are expressed in alveolar type II and human lung tumor cells. Rats with higher dopaminergic activity developed smaller tumor and fewer lung metastases than rats with low dopaminergic activity [28]. By maintenance of tissue energy content, ADORA1 agonists reduced LPS-induced vasoconstriction and oedema formation. Thus, adenosine receptor stimulation might be beneficial during acute lung injury [29]. On the other hand, alcohol decreases alveolar fluid clearance and impairs survival from acute lung injury, and it induced the increasing level in lung adenosine levels responsible for the reduction of alveolar fluid clearance and worsening of lung injury [30]. Therefore, the pathway of neuroactive ligand–receptor interaction and alcoholism may act synergistically in the treatment of JZ. For the rest, drug metabolic process, lung development and the metabolic pathways indicated that intervention with metabolic process might play a significant role in lung injury.

Through existing detection methods, the components related to Caprae Hircus Cornu, Chloriti Lapis and Gypsum Fibrosum cannot be detected, which limited the further analysis.

4. Conclusions

In this paper, UPLC-Q-TOF/MS technology was used to analyze the chemical constituents in plasma, urine, feces and bile of rats treated with JZ. And a total of 31 prototype constituents and 41 metabolites were detected or identified. Hydroxylation, sulfation and glucuronidation were the main metabolic reactions. The further absorbed constituent-target-disease network was generated to illustrate the relationship among 72 compounds, 24 potential targets and 15 related metabolites. These results reveal the major absorption components and metabolic pathways of JZ. More importantly, the potential therapeutic targets and biological processes may provide valuable information for further investigation into the new therapeutic mechanisms of JZ.

Conflicts of interest

Authors have no conflict of interest.

Acknowledgements

The work was supported by State Key Laboratory of Pharmaceutical New-tech for Chinese Medicine (SKL2010M0202-001), the National Natural Science Foundation of China (81470176), Overseas Training Project of Liaoning Colleges and Universities (2018LNGXGJWPY-YB024) and the Project of Science and Technology of the Education Department of Liaoning Province (2017LQN11).

Appendix A. Supplementary data

Supplementary data to this article can be found online at https://doi.org/10.1016/j.jfda.2019.05.007.

REFERENCES

[1] Peng W, Jin F, Chen C. The clinical observation of the treatment of Mycoplasma pneumoniae pneumonia with Jinzhen oral liquid and clarithromycin. Zhongyi Er Ke Za Zhi 2012;8:15–8 [in Chinese].
[2] Zong SB, Sun L, Yao-Zhong L, Zhou J, Wang ZZ, Wei X. Effect of Jinzhen oral liquid on NF-κB,MAPK signaling pathway in mice with LPS-induced acute lung injury. Zhongguo Shi Yan Fang Ji Xue Za Zhi 2018;24:155–9 [in Chinese].
[3] Liu XQ, Fu YY, Xu JJ, Pan YN, Wang ZZ, Xiao W. Study on quality standard of Jinzhen Oral liquid. Zhongguo Xian Dai Zhong Yao 2013;15:987–91 [in Chinese].
[4] Wang CH, Zhong Y, Zhang Y, Liu JP, Wang YF, Jia WN, et al. A network analysis of the Chinese medicine Lianhua-Qingwen formula to identify its main effective components. Mol Biosyst 2016;12:606–13.
[5] Shao L. Network target:a starting point for traditional Chinese medicine network pharmacology. Zhongguo Zhongyao Zazhi 2011;36:2017–20 [in Chinese].
[6] Zhang X, Pi Z, Zheng Z, Liu Z, Song F. Comprehensive investigation of in-vivo ingredients and action mechanism of iridoid extract from Gardeniae Fructus by liquid chromatography combined with mass spectrometry, microdialysis sampling and network pharmacology. J Chromatogr B Analyt Technol Biomed Life Sci 2018;1076:70–6.
[7] Michael K, Christian VM, Monica C, Lars Juhl J, Peer B. STITCH: interaction networks of chemicals and proteins. Nucleic Acids Res 2008;36:684–8.
[8] David G, Aurélien G, Matthias W, Antoine D, Olivier M, Vincent Z. SwissTargetPrediction: a web server for target prediction of bioactive small molecules. Nucleic Acids Res 2014;42:32–8.
[9] Chen X, Ji ZL, Chen YZ. TTD: therapeutic target database. Nucleic Acids Res 2002;30:412–5.
[10] Ada H, Alan FS, Joanna SA, Carol AB, Victor AM. Online Mendelian Inheritance in Man (OMIM), a knowledgebase of human genes and genetic disorders. Nucleic Acids Res 2005;33:514–7.
[11] Piñero J, QueraltRosinach N, Bravo À, DeuPons J, BauerMehren A, Baron M, et al. DisGeNET: a discovery platform for the dynamical exploration of human diseases and their genes. Database (Oxford) 2015;15:bav028.
[12] Wishart DS, Craig K, An Chi G, Dean C, Savita S, Dan T, et al. DrugBank: a knowledgebase for drugs, drug actions and drug targets. Nucleic Acids Res 2008;36:901–6.
[13] Da WH, Brad TS, Richard AL. Bioinformatics enrichment tools: paths toward the comprehensive functional analysis of large gene lists. Nucleic Acids Res 2009;37:1–13.
[14] Lambert M, Stærk D, Hansen SH, Sairafianpour M, Jaroszewski JW. Rapid extract dereplication using HPLC-SPE-

NMR: analysis of isoflavonoids from *smirnowia iranica*. J Nat Prod 2005;68:1500–9.
[15] Lee YP, Kuo TF, Lee SS. Identification of the metabolites of TCM prescription Sinisan, found in miniature pig urine via intragastric administration. J Pharm Biomed Anal 2015;111:311–9.
[16] Liu C, Zhou S, Begum S, Sidransky D, Westra WH, Califano JA. Increased expression of repair genes TDP1 and XPF in human lung cancers. Cancer Res 2006;47:193.
[17] Satoshi E, Toshiyuki M, Hiroaki M, Chisato O, Midori S, Yukio K, et al. Kinetic studies of AKR1B10, human aldose reductase-like protein: endogenous substrates and inhibition by steroids. Arch Biochem Biophys 2009;487:1–9.
[18] Giménez-Dejoz J, Kolář MH, Ruiz FX, Crespo I, Cousido-Siah A, Podjarny A, et al. Substrate specificity, inhibitor selectivity and structure-function relationships of aldo-keto reductase 1B15: a novel human retinaldehyde reductase. PLoS One 2015;10:e0134506.
[19] Wu F, Li WW, Song Y, Chen L, Shi Y, XZ H. Experimental study on the changes of A549 autophagy signal induced by deoxycholic acid in alveolar epithelial cells induced by glargine geese. Zhongguo Ji Jiu Fu Su Yu Zai Hai Yi Xue Za Zhi 2015;2:119–21 [in Chinese].
[20] Andrea W, Harald K, Nicole B, Szolar OHJ. Glycyrrhizin inhibits influenza A virus uptake into the cell. Antivir Res 2009;83:171–8.
[21] Bolt RJ, Van Weissenbruch MM, Lafeber HN, Waal DVD. Glucocorticoids and lung development in the fetus and preterm infant. Pediatr Pulmonol 2010;32:76–91.
[22] Maser E, Oppermann UC. Role of type-1 11beta-hydroxysteroid dehydrogenase in detoxification processes. Eur J Biochem 1997;249:365–9.
[23] Augustin B, Michèle G, Véronique B, Alexandre M, Robert B, Francelyne M, et al. Involvement of reactive oxygen species in the metabolic pathways triggered by diesel exhaust particles in human airway epithelial cells. Am J Physiol Lung Cell Mol Physiol 2003;285:671–9.
[24] Thannickal VJ, Fanburg BL. Reactive oxygen species in cell signaling. Am J Physiol Lung Cell Mol Physiol 2000;279:L1005–28.
[25] Yi G, Liang M, Li M, Fang X, Liu J, Lai Y, et al. A large lung gene expression study identifying IL1B as a novel player in airway inflammation in COPD airway epithelial cells. Inflamm Res 2018;67:1–13.
[26] Novikova VA, Nia I, Soldatova AP. Use of steroid hormones in the complex therapy of chronic pneumonia in children. Vopr Okhr Materin Det 1965;10:50–3.
[27] Blackburn MR, Volmer JB, Thrasher JL, Zhong H, Crosby JR, Lee JJ, et al. Metabolic consequences of adenosine deaminase deficiency in mice are associated with defects in alveogenesis, pulmonary inflammation, and airway obstruction. J Exp Med 2000;192:159–70.
[28] Teunis MAT, Annemieke K, Emile V, Bakker JM, Ellenbroek BA, Cools AR, et al. Reduced tumor growth, experimental metastasis formation, and angiogenesis in rats with a hyperreactive dopaminergic system. FASEB J 2002;16:1465–7.
[29] Heller AR, Rothermel J, Weigand MA, Plaschke K, Schmeck J, Wendel M, et al. Adenosine A1 and A2 receptor agonists reduce endotoxin-induced cellular energy depletion and oedema formation in the lung. Eur J Anaesthesiol 2007;24:258–66.
[30] Laura D, Gonzalez AR, Daniela U, Saul S, Manghi TS, Chiarella SE, et al. Alcohol worsens acute lung injury by inhibiting alveolar sodium transport through the adenosine A1 receptor. PLoS One 2012;7:e30448.